Contract No:

This document was prepared in conjunction with work accomplished under Contract No. DE-AC09-08SR22470 with the U.S. Department of Energy.

Disclaimer:

This work was prepared under an agreement with and funded by the U.S. Government. Neither the U. S. Government or its employees, nor any of its contractors, subcontractors or their employees, makes any express or implied: 1. warranty or assumes any legal liability for the accuracy, completeness, or for the use or results of such use of any information, product, or process disclosed; or 2. representation that such use or results of such use would not infringe privately owned rights; or 3. endorsement or recommendation of any specifically identified commercial product, process, or service. Any views and opinions of authors expressed in this work do not necessarily state or reflect those of the United States Government, or its contractors, or subcontractors.

NATURAL CIRCULATION IN HEAT REMOVAL SYSTEM DURING LOSS-OF-PUMP ACCIDENT BASED ON INITIAL CONCEPTUAL DESIGN

S. Y. Lee[*], L. L. Hamm[+], and F. G. Smith, III[%]
Savannah River National Laboratory
Aiken, SC 29808
Tel: (803) 725-8462
Fax: (803) 725-0141
[*]si.lee@srnl.doe.gov, [+]luther.hamm@srnl.doe.gov, [%]frank02.smith@srnl.doe.gov

ABSTRACT

A transient natural convection model of the accelerator blanket primary heat removal (HR) system was developed to demonstrate that the blanket could be cooled for a sufficient period of time for long term cooling to be established following a loss-of-flow accident (LOFA). The particular case of interest in this work is a complete loss-of-pumping accident. For the accident scenario in which pumps are lost in both the target and blanket HR systems, natural convection provides effective cooling of the blanket for approximately 68 hours, and, if only the blanket HR systems are involved, natural convection is effective for approximately 210 hours. The heat sink for both of these accident scenarios is the assumed stagnant fluid and metal on the secondary sides of the heat exchangers.

KEYWORDS
Natural Circulation Cooling Model, Loss-Of-Flow Accident, Decay Heat Cooling

1. INTRODUCTION

Loss of power could leave the Accelerator Target/Blanket (T/B) Facility without running pumps resulting in no forced circulation in the primary and secondary heat removal systems for an extended period of time. Natural circulation (NC) would occur in the primary HR system; however, without circulation through the secondary sides of the heat exchangers there would not be an ultimate heat sink for the decay power in the blanket modules. To prevent some or all of the blanket modules from eventually overheating and losing structural integrity, either power would have to be restored or the cavity flood system would have to be activated. There would be a period of time following the loss of forced convection in the HR systems when the modules would be cooled by natural convection. The stagnant water in the secondary sides of the heat exchangers could serve as a temporary heat sink, diminishing in effectiveness as it heats up. A transient single-phase natural convection model of the primary HR system was developed to determine the duration of time of effective passive cooling of the modules. A special purpose FORTRAN program was developed, called NCLOFA.

The accident under consideration is a facility loss-of-power that results in the simultaneous loss of both the T/B primary and secondary coolant pumps. This accident is unmitigated except for a beam shutdown. The primary HR systems would ultimately dry out by boiling off the coolant inventories, if corrective action is not taken. This would occur much sooner in the target system

than the blanket because of the differences in both metal and coolant masses. The target can survive high temperatures where thermal radiation to the blanket is an acceptable heat removal mechanism; whereas, without cavity flooding, the blanket cannot maintain its structural integrity very long after dryout. Based on results presented in Ref. [1], the target is assumed to dry out twenty four hours after the onset of the accident and the target decay power is then deposited in the Module 1 decouples. The model is run until the HR system coolant reaches its saturation temperature. Beyond this point two-phase flow is established; however, the NC model chosen for this set of analyses is limited to single-phase conditions. Even though it is anticipated that significant cooling capability further exists once boiling begins. No formal credit for boiling capability is taken at this time, since a significant increase in modeling complexity would only extend the existing acceptable period of time available prior to taking corrective action. The consequences of this accident scenario envelop those of the scenario where only the blanket primary and secondary coolant pumps are lost.

2. DESCRPTION OF THE MODEL

The transient single-phase NC model of the primary HR system is based on a flow network with three lumped modules and one lumped heat exchanger, as shown in Fig. 1. The three lumped modules constitute three parallel legs between the fixed inlet and outlet headers, and the heat exchanger is in a fourth leg that forms the network into a closed loop. The various legs of the flow network that make up the NC model represent lumped flow paths. The accelerator T/B facility consists of the 16 module cruciform-type units in the current blanket design (see Ref. [2] for further details). These modules are combined into lumped f!ow paths (referred to as legs) as listed below:

- “Leg 1”– the lateral Row-1/ decoupler modules listed as Modules 1 and 4;
- “Leg 2“ – the remaining vertical modules listed as Modules 2, 3, 5, 6, 7, 8, and 9;
- “Leg 3“ – all horizontal modules listed as Modules 10, 11, 12, 13, 14, 15, and 16;
- “HXLeg”– blanket primary HR loop containing the two heat exchangers, two pumps, and piping from the outlet header back around to the inlet header closing the flow network.

The labels above are also provided in Fig. 1. The pressurizer is not modeled explicitly but does establish the network reference pressure at the inlet header. The heated upflow and downflow sections of a module are treated separately in the momentum equations, and the impact of buoyancy-assisted/opposed mixed convection flow is accounted for through a Rayleigh number dependent modification of the Darcy friction factor. The heated solid sections of the modules are lumped together with the coolant flowing through them in the thermal energy equations. The aluminum clad lead plates and the fluid in the adjacent channels are assumed to be isothermal. This is reasonable at the low metal power densities encountered under post beam shutdown conditions and with the high heated surface area to fluid volume ratios for the flow channels. This simplification avoids the necessity of solving conjugate heat transfer problems within the modules. There are four momentum equations, one for each leg in the loop and a continuity equation for the outlet header. These five equations are solved simultaneously for the four leg mass flowrates and the outlet header pressure each time step using a standard Newton-Raphson method. The inlet header pressure is a boundary condition that specifies the system reference pressure.

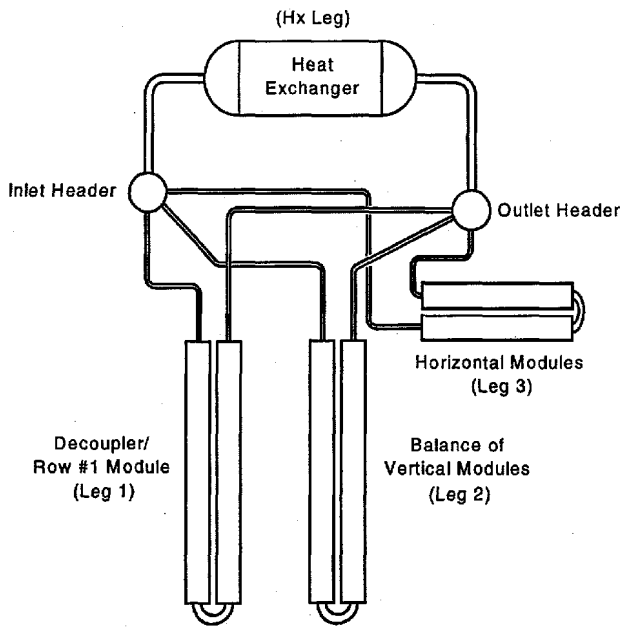

Figure 1. Schematic of the blanket primary heat removal system with three lumped modules and one lumped heat exchanger loop.

For determining the transient temperature distribution within the network, each of the module legs of the network is divided into five cells, while the heat exchanger leg is divided into three. Under low flow conditions for which this model is intended, this spatial resolution is adequate. A thermal energy equation is derived for each leg cell, each of the headers, and for the shell (or secondary) side of the heat exchanger. The energy equations are difference in time allowing a varying degree of implicitness specified by the user. The energy equations are solved iteratively each time step in a two-step process. The two header temperatures and the temperature on the secondary side of the heat exchanger are updated. With these updated values, the network leg temperatures are updated by marching in the flow direction from the upstream to the downstream header for each leg. This process is repeated until convergence occurs. The momentum and thermal energy equations are derived in Appendix A. The natural circulation is driven by the time dependent decay power in the heated sections of the module legs. After 24 hours have elapsed, the total target decay power is deposited in the decoupler section of Leg 1. This is the heated section in Leg. 1 closest to the inlet header. This additional power is ramped in over a period of one hour. The NC simulation commences one hour after the onset of the accident and continues until the primary coolant reaches its saturation temperature. The model predicts the transient mass flowrates in the network legs, the outlet header pressure, the transient temperature distribution in the primary coolant, and the shell side heat exchanger temperature. Appendix C contains a sample-input file and Appendix D contains a code listing of the NCLOFA program.

The Darcy friction factors for mixed forced/free laminar convection through vertical passages can differ significantly from the forced convection values defined as sixty-four over the Reynolds number. In upflow through a heated vertical channel, buoyancy flattens the parabolic radial velocity profile and increases the wall velocity gradient, thereby, increasing the wall shear. In downflow, buoyancy decreases the radial velocity gradient at the wall and therefore the wall

shear. The friction factor for heated upflow is increased, and for downflow it is decreased. No effect exists for horizontal flow paths. Based on a plot of Fanning friction factors for buoyancy assisted and retarded flows between vertical flat plates in Ref. [3], correlations were developed for friction factor multipliers as functions of a modified Rayleigh number. These correlations are developed in Appendix B. They are used in the NC model to modify the friction factors in the heated sections of the two network vertical module legs.

3. RESULTS AND DISCUSSION

Two facility loss-of-power accident scenarios were simulated with the normal operation (NO) model: a simultaneous loss of both the T/B primary and secondary coolant pumps, and a loss of only the blanket primary and secondary coolant pumps. The first scenario is the more interesting of the two because flow reversals occur. It is also the more limiting ease because, with the addition of the target decay power, more power (approximately double) is transferred to the coolant. The results of this accident simulation are described first and in detail. The results for the latter scenario are described primarily by comparison and contrast with the results of the former.

Figure 2 shows, for the first accident scenario, the network mass flowrates for the three modules and the heat exchanger leg as functions of elapsed time. By definition, positive flow through the three module legs travels from the inlet header to the outlet header and return flow occurs through the heat exchanger leg. During normal operation and prior to the depositing of the target power in the decoupler, the flow is positive throughout the network. The target is assumed to dry out within twenty-four hours of the onset of the accident, and thereafter, the target decay power is dissipated by thermal radiation to the cooler adjacent blanket system decouples. The blanket decouples virtually surround the ladder assemblies, neutronically decoupling the target from the lead blanket. It is assumed that all thermal radiation emanating from the target ladders is deposited into the decoupler. This power is assumed to be ramped jn over a period of one hour. With the addition of the target power, significantly more power is dissipated in the decoupler than in the Row-1 section of Leg 1, and buoyancy causes a flow reversal to occur. Deposited power levels under NO conditions are given in Table I.

Figure 3 shows an expanded view of the network mass flowrates during the period in which the flow reversals occur. Shortly after the flow reversal occurs in Leg 1 of the network, the flows reverse in Leg 3 and the Hx leg. The flow does not reverse in Leg 2. There are no preferred flow directions, due to buoyancy, in Leg 3 and the Hx leg of the network, so the flows in these legs readily reverse as consequences of the flow reversal in Leg 1. Buoyancy dictates the flow direction in Leg 2, and since the relative power distribution in this module doesn’t change, neither does its flow direction.

Figure 4 shows the temperatures of the two headers and the shell side of the heat exchanger. Prior to the flow reversals, the inlet header is colder than the outlet header, which is to be expected since the flows in all three modules are positive. After the flow reversals, the outlet header is colder than the inlet header. The shell side of the heat exchanger has the lowest of the three temperatures. This is the system heat sink. The increased heating rate of the fluid after the target power is deposited in the decoupler is evident from the slopes of the transient temperature plots.

Table I Normal operation deposited power levels.

Nat. circulation model ID	Decay power (MW) (NO downflow section)	Decay power (MW) (NO upflow section)
Leg 1	8.222	15.768
Leg 2	9.083	17.695
Leg 3	0	5.712
HX Leg	0	0
Totals	56.48 (blanket) 68.01 (targets)	- -

Figures 5 through 7 show the two header temperatures and the temperatures in the two heated sections of each of the three legs, respectively. Figure 8 shows the two header temperatures and the heat exchanger temperature. The effects of the flow reversals on the relative magnitudes of the temperatures in the heated sections of legs one and three are evident. The flow does not reverse in Leg 2, and therefore, the downstream heated section remains hotter than the upstream heated section throughout the accident scenario. These two temperatures exceed the inlet header temperature after the flow reversals because the flow in this leg occurs from the inlet header to the outlet header. The highest system temperature occurs in this module. The heat exchanger primary (or tube side) temperature is equal to the inlet header temperature prior to the flow reversals, and it is slightly lower than the outlet header temperature after the flow reversals. After the flow reversals, the outlet header temperature is slightly greater than the heat exchanger temperature because Leg 2 continues to discharge into the outlet header.

Figure 9 shows the transient outlet header pressure. It is constant at 107.3 psia, given a specified inlet header pressure of 106.24 psia. The difference between the two pressures is hydrostatic.[n each leg of the network, the net buoyant force balances the dynamic pressure drop force. At the inlet header pressure the saturation temperature is 166.8°C and the inlet header reaches this temperature 67.9 hours after the onset of the accident. Once the mean fluid temperature reaches saturation, bulk boiling will commence and the system will start to pressurize. The primary and secondary coolants will continue to heat up as the saturation temperatures increase due to system pressurization. Since pressurizing the primary blanket HR system would threaten its integrity, bulk boiling should be avoided. The point at which the primary coolant temperature reaches saturation is defined as the limit of effective natural convection cooling by the blanket HR system.

If the LOFA is confined only to the blanket HR system, the period of adequate natural convection cooling under single-phase flow is significantly longer than for the scenario just considered, in which both the target and blanket systems are involved. As Table 2 shows, the blanket only constitutes about 45% of the total deposited power being generated in the T/B facility. Figure 10 shows the mass flowrates in the three legs and the Hx leg of the NC network. The flowrates decrease monotonically due to the decay of the internal heat generation in the blanket modules. There is no flow reversal because the relative power distribution within the blanket modules remains constant. Figure 11 shows the transient fluid temperatures in the inlet header, outlet header, and on the shell side of the heat exchanger. Approximately 210 hours are

required for the fluid in the outlet header to reach its saturation temperature of 167.2C. This is considerably longer than 68 hours of effective natural convection cooling in the accident scenario that involves the target.

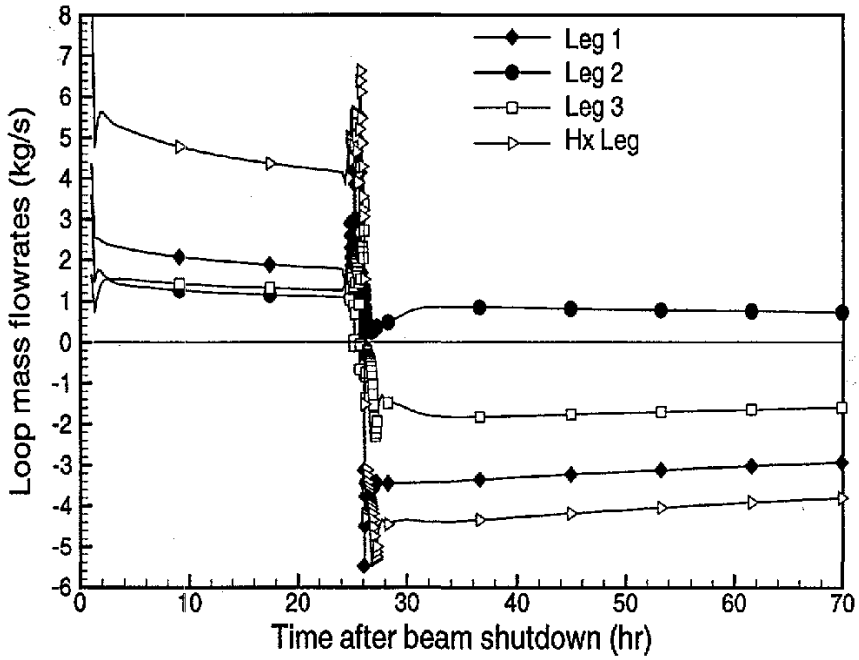

Figure 2. Natural circulation flowrates during a primary and secondary loss of flow accident (LOFA).

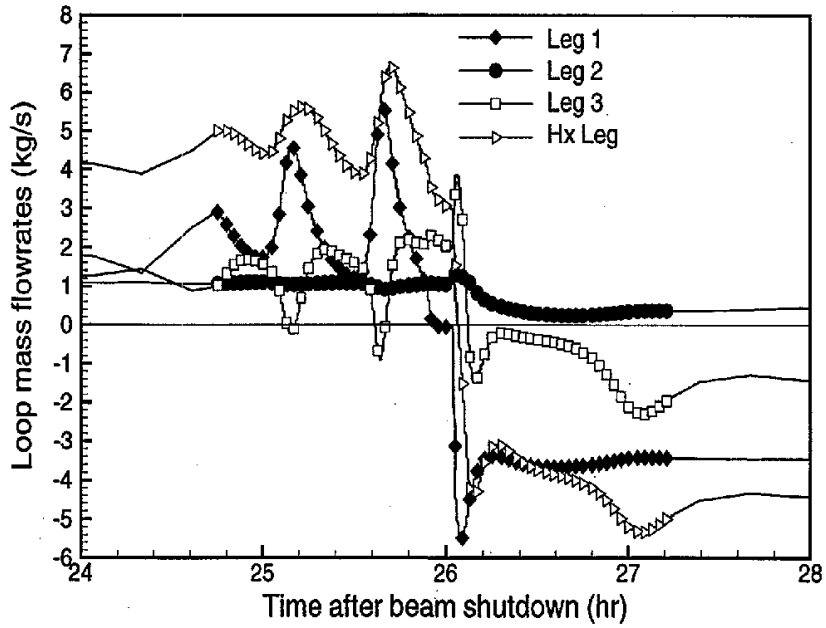

Figure 3 Expanded view of the flowrates during the flow reversal process.

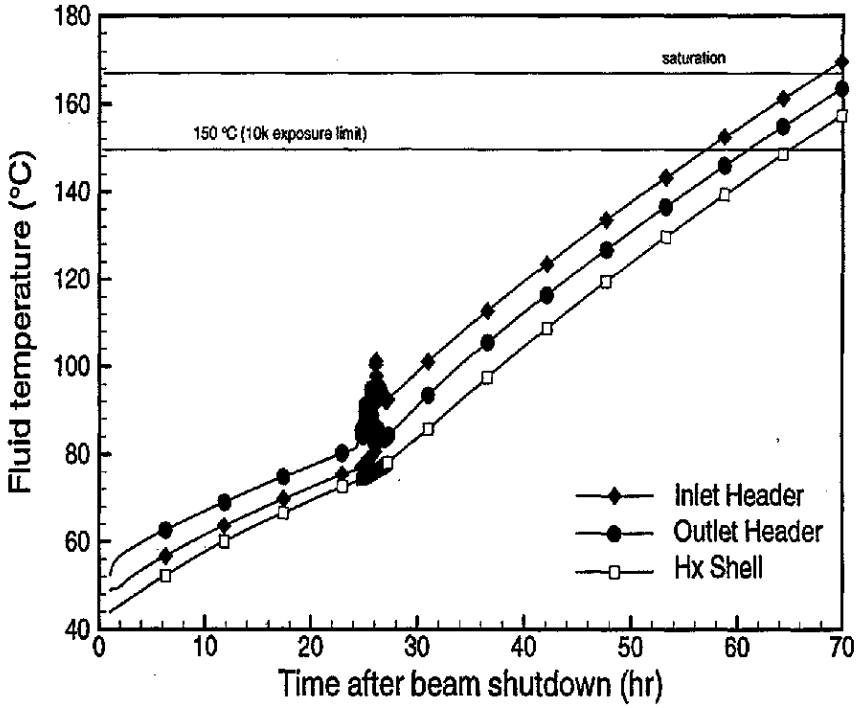

Figure 4 Transient fluid temperatures of the two headers and the shell side of the heat exchanger during LOFA.

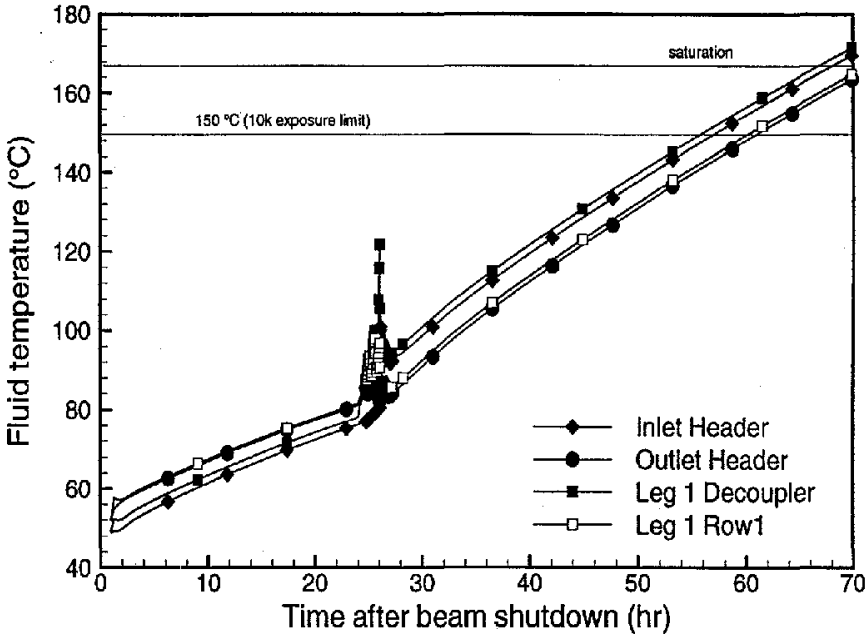

Figure 5 Transien1t temperatures in the headers and Leg 1 during a T/B LOFA.

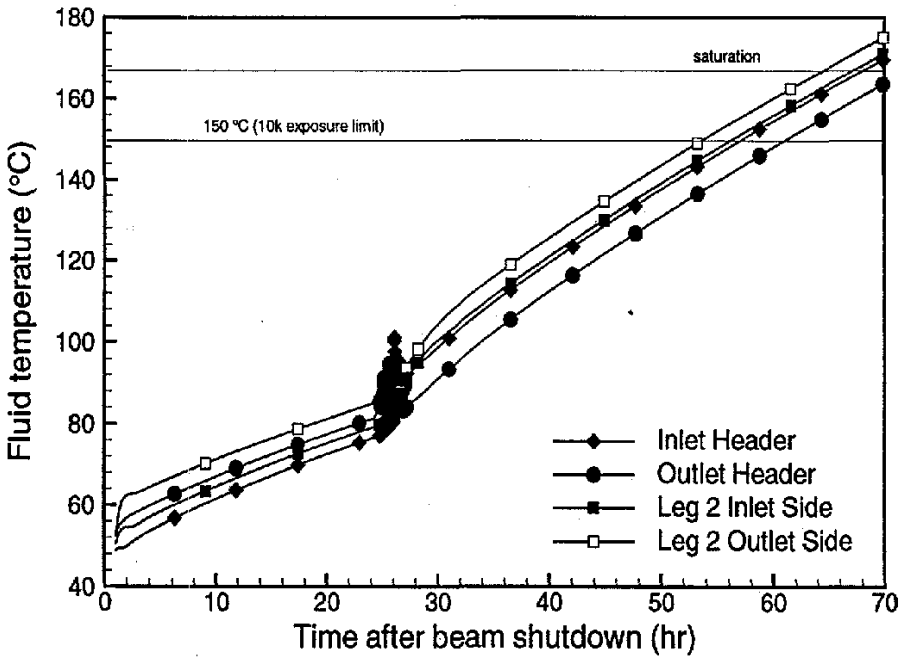

Figure 6 Transient temperatures in the headers and Leg 2 during a T/B LOFA.

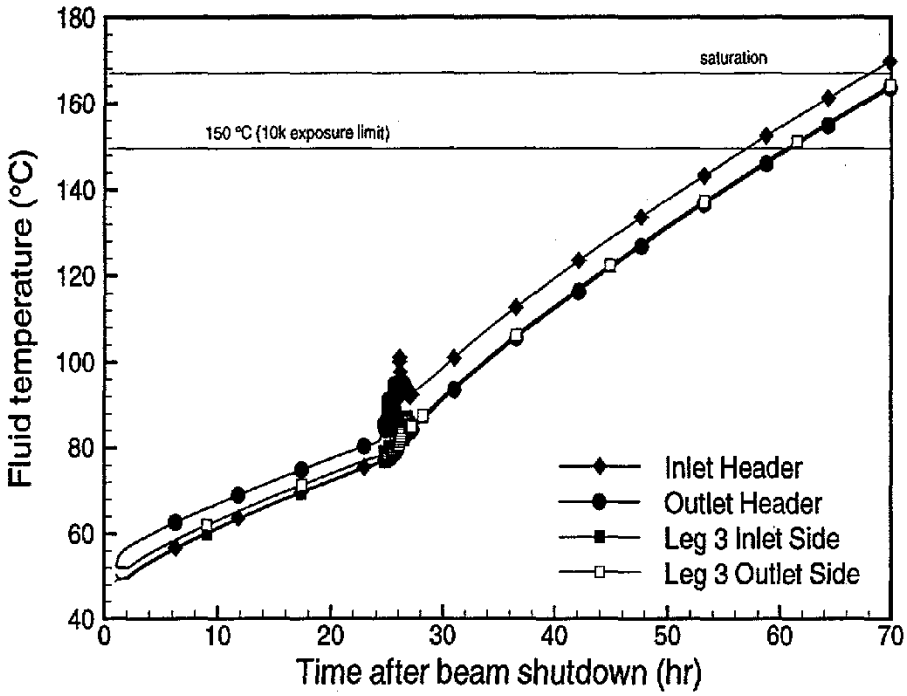

Figure 7 Transient temperatures in the headers and Leg 3 during a T/B LOFA.

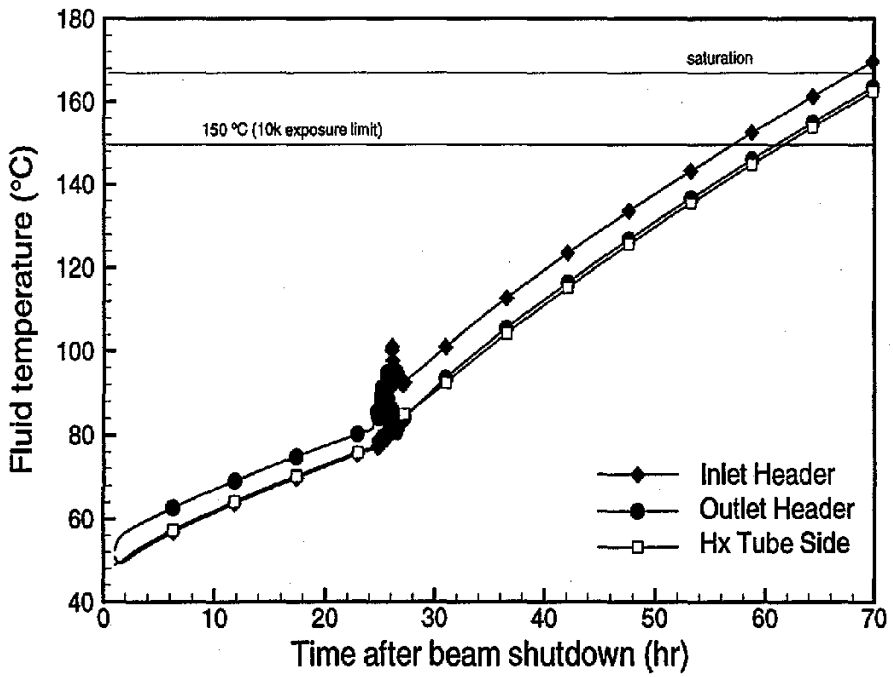

Figure 8 Transient temperatures in the headers and the tube side of the heat exchanger during a T/B LOFA.

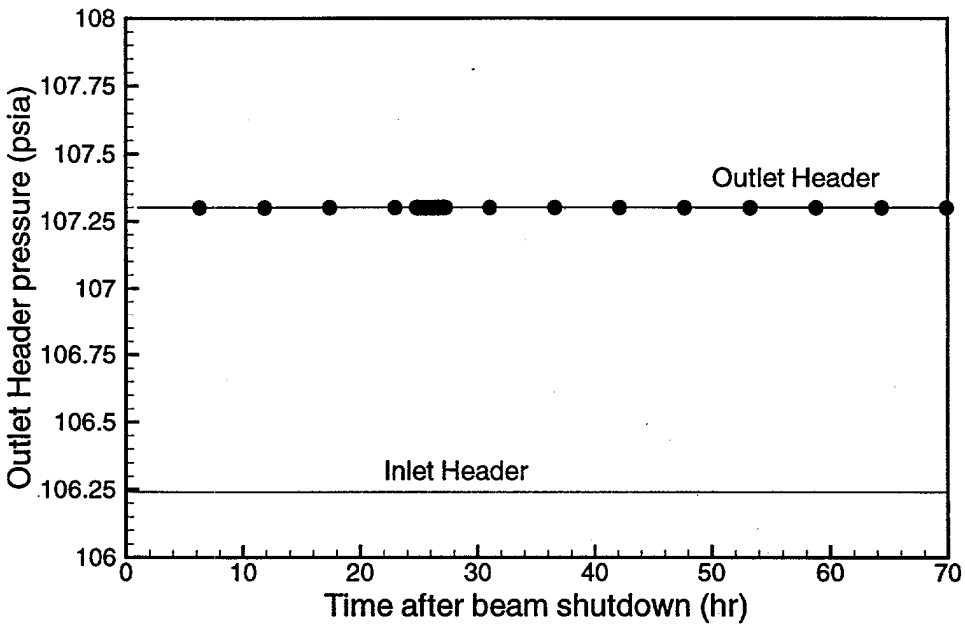

Figure 9 Outlet header pressure during a T/B LOFA.

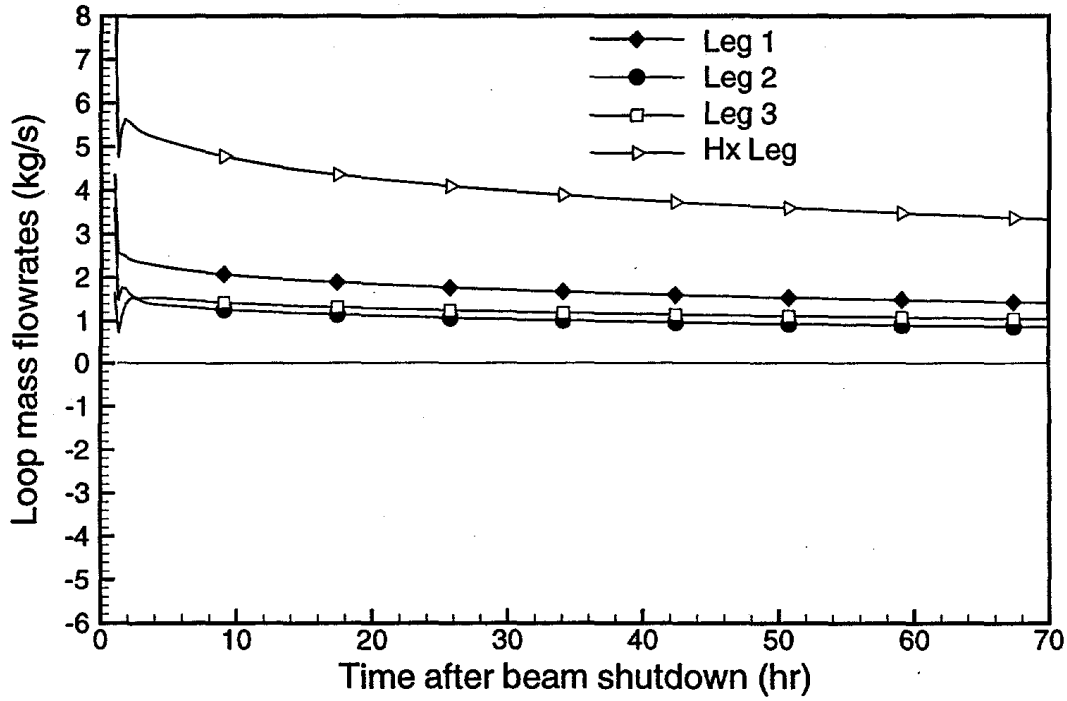

Figure 10 Natural circulation flowrates during a blanket only LOFA.

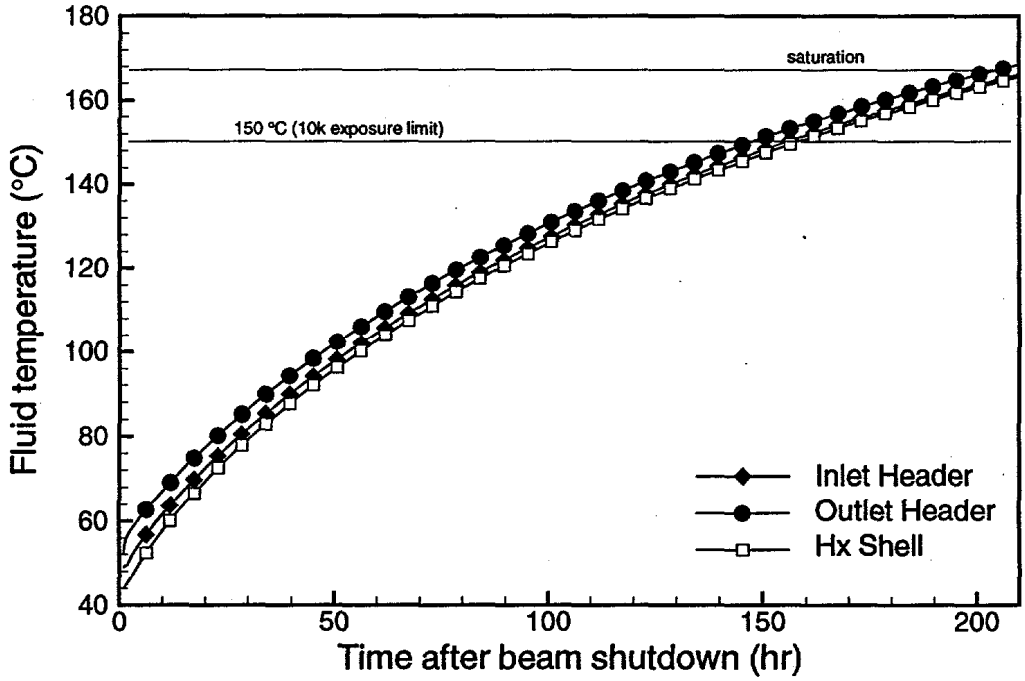

Figure 11 Transient fluid temperatures in the two headers and the shell side of the heat exchanger during a blanket only LOFA.

4. CONCLUSIONS

The period of effective single-phase natural convection cooling of the accelerator blanket, following a facility loss-of-power accident that results in the simultaneous loss of both the target and blanket primary and secondary pumps, is approximately 68 hours. This is the time required for the coolant to reach its saturation temperature. The transient heat sink for this accident scenario is the stagnant fluid in the shell side of the heat exchanger. If the target HR system is not involved in this accident scenario, the period of effective natural convection cooling is extended to approximately 210 hours. These are the allowable time periods available for restoring electrical power to the pumps or establishing an alternate means for cooling the blanket assemblies.

The volume of assumed stagnant water on the shell sides of the heat exchangers and the masses of metal in the heat exchangers are the heat sinks for the NC model. Other than sensible heating, no other phenomena with respect to the shell side of the heat exchanger were considered in this accident analysis. If the pressure in the blanket secondary HR system is less than that in the primary system, the secondary side fluid would boil before the primary fluid reached saturation. This probably will not be the case since maintaining the secondary side heat exchanger pressure at a higher value than the primary side is desirable for radionuclide containment. This aspect of the accident analysis does warrant further consideration. Boiling on the secondary side could provide effective cooling for a while, but the heat sink would completely lose its effectiveness after dryout. The fluid in the secondary HR system could also circulate by natural convection, thereby, extending the period of time that the system is an effective heat sink for the primary HR system.

REFERENCES

1. W. R. Bohland, K. O. Pasamehmetoglu, "Temperature Calculationsfor a Dry-Rung in a Dry or Flooded Cavity after a LOFA or a LOCA in the Tungsten Neutron Source Primary l-feat Removal System," Los Alamos National Laboratory calcnote, CN-APT/TSAl 0-005, February (1998).
2. L. L. Hamm, S. Y. Lee, M. A. Shadday, and F. G. Smith, Ill, "APT Blanket System Model Based On Initial Conceptual Design - Integrated 1D TRAC System Model," Westinghouse Savannah River Company, WSRC-TR-98-O053 (July 1998).
3. S. Kakac, R. K. Shah, and W. Aung, "*Handbookof Single-phase Convective Heat Transfet*', John Wiley& Sons (1987).

APPENDIX A: DERIVATION OF THE GOVERNING EQUATIONS

The primary HR system flow network consisting of three lumped legs, as shown in Fig. A-1, is divided up into several interconnected discrete control volumes. To derive the governing equations for transient single-phase natural convection for this simplified model, the incompressible continuity, momentum, and thermal energy equations were applied to the control volumes. A Boussinesq fluid was assumed to handle the buoyancy terms in the momentum equations. Four momentum equations, one for each leg, and the continuity equation for the outlet header are solved simultaneously for the mass flowrates in each leg and the outlet header pressure. The thermal energy equations for the header temperatures, the heat exchanger shell side temperature, and the temperature distributions within each network leg are solved separately from the momentum equations.

Figure A-2 shows one of the lumped module legs of the network and a close up of a representative control volume of one of the sections of the leg. The external forces acting on the fluid in the control volume are shown. They are the normal facing pressure forces, the body force, and the wall shear (or frictional force). The linear momentum equation (Eq. a1) is applied to each of the five control volumes within a leg. Equation a2 is the body force term and Eq. a3 is the frictional force term. The "n" in the subscript refers to the leg number, and the second number refers to the cell number, one through five. Equation a4 is the momentum equation for the first cell of the leg.

There are four additional equations, one for each of the other cells. If the area changes between cells are neglected, the five momentum equations can be added together to yield a single leg momentum equation (Eq. (a5)) with the header pressures and the leg mass flowrate as unknowns. At the low flowrates expected under natural convection conditions, the pressure distributions in the network legs will be close to hydrostatic. The flow area expansions and contractions occur in pairs with the same elevation, points 2 and 5 and points 3 and 4 in Fig. A-1. For these reasons the area changes can be neglected. The alternative would be to calculate intermediate pressures at the cell faces, and this would significantly increase the number of simultaneous non-linear equations to be solved and from an accuracy perspective is not warranted.

$$\frac{d}{dt}(m\bar{v}) + \dot{m}(\bar{v}_{out} - \bar{v}_{in}) = \sum \vec{F} \tag{a1}$$

$$F_B = \rho_o[1 - \beta(T_{n1} - T_o)]A_{n1} g \Delta z_{n1} \tag{a2}$$

$$F_f = \frac{f_{n1} L_{n1} \dot{m}_n^2}{2\rho_o D_{n1} A_{n1}} \tag{a3}$$

$$L_{n1}\frac{d\dot{m}_n}{dt} = F_B + F_f + P_1 A_{n1} - P_2 A_{n2} \tag{a4}$$

$$\sum_i L_{ni}\frac{d\dot{m}_n}{dt} = \sum_i (F_{Bni} + F_{fni}) + P_{in} A_{n1} - P_{out} A_{n5} \tag{a5}$$

where

F = force
P = fluid density
f = Darcy friction factor
m = mass flowrate
β = coefficient of thermal expansion
P = pressure
A = flow area
T = temperature
L = cell length
g = gravitational constant
D = hydraulic diameter
Δz = elevation difference

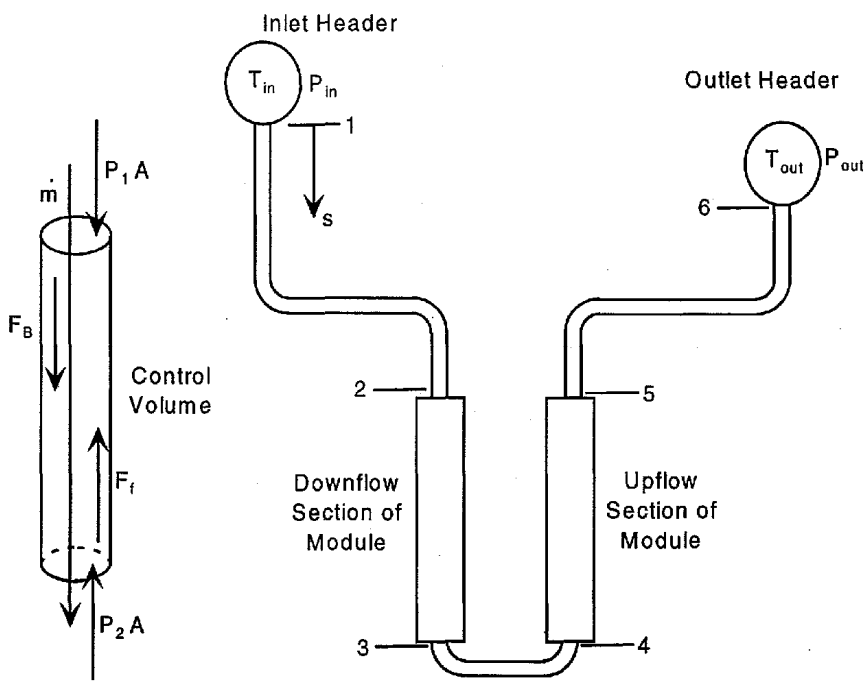

Figure A-1. Schematic of one of the module legs of the natural convection network showing the control volumes used to derive the momentum equation.

Figure A-2 shows a schematic of the network leg that contains the heat exchanger. This leg is divided into three sections. The overall momentum equation for the mass flowrate in this leg is derived in the same manner as the equations for the module legs.

Figure A-3 *is* a schematic of the outlet header that shows the mass flowrates entering and exiting the header. Positive flowrates are shown. The continuity equation is applied to the control volume to yield Eq.a6. This equation and the four network leg momentum equations are solved simultaneously each time step for the leg mass flowrates and the outlet header pressure. The inlet header pressure is a boundary condition.

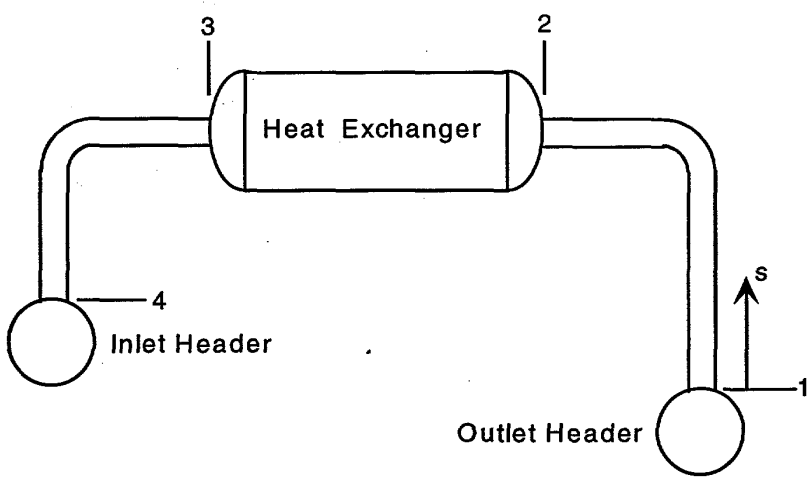

Figure A-2. Schematic of the heat exchanger leg of the natural convection network.

A mixed implicit/explicit scheme is used to derive the thermal energy equations. A separate equation is derived for each cell of the network legs and for each header. There is also an energy equation for the secondary side of the heat exchanger. Equation (a7) is the thermal energy equation for the second cell of the module leg shown in Fig. A-2. This cell is the downflow section of the heated module. Upwind differencing is used, and Eq. (a7) applies to the case with positive flow. With negative flow the convective terms would be appropriately modified. The value of the coefficient "α" determines the degree of implicitness of the equation. The equation is fully implicit with "α" set equal to one and fully explicit with "α" set equal to zero. A value of one-half results in the Crank Nicholson scheme. The superscript "n" denotes the new time level. Equation (a8) is the expression for the updated nodal temperature. Note that only upstream temperatures at the new time level appear on the right-hand-side of the equation. Therefore, the temperatures in a specified leg of the network can be updated in a marching scheme starting at its upstream header.

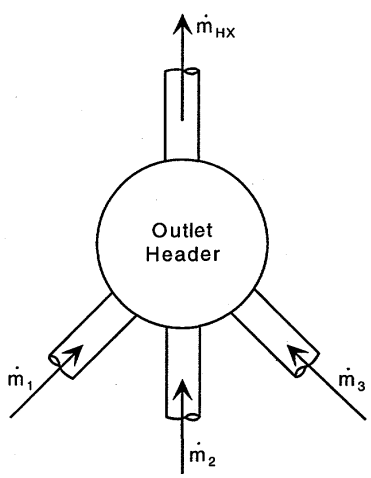

Figure A-3. Schematic of the outlet header showing the mass flowrates

$$\dot{m}_1 + \dot{m}_2 + \dot{m}_3 - \dot{m}_{Hx} = 0 \tag{a6}$$

$$(m_s + m)\overline{C}_p \frac{T_{n2}^n - T_{n2}}{\Delta t} = \dot{m}_n C_p \left[\alpha T_{n1}^n + (1-\alpha)T_{n1}\right] - \dot{m}_n C_p \left[\alpha T_{n2}^n + (1-\alpha)T_{n2}\right] + \dot{Q}_{n2}(t) \tag{a7}$$

$$T_{n2}^n = \frac{\frac{(m_s+m)\overline{C}_p}{\Delta t} T_{n2} + \dot{m}_n C_p \left[\alpha T_{n1}^n + (1-\alpha)T_{n1}\right] - \dot{m}_n C_p (1-\alpha)T_{n2} + \dot{Q}_{n2}(t)}{\frac{(m_s+m)\overline{C}_p}{\Delta t} + \alpha \dot{m}_n C_p} \tag{a8}$$

where

m = fluid mass

m_s = solid (metal) mass

C_p = fluid specific heat

$\overline{C}_p$ = mass weighted liquid/solid composite specific heat

$\dot{Q}_{n2}(t)$ = deposited decay heat for cell n2

α = implicitness parameter

Δt = time step size

Similar equations can be derived for the remaining cells of the module leg shown in Fig. A-1. The storage terms for the two heated cells represent both the masses of the lead/aluminum metal and the fluid in the channels. Their specific heats are composite values. There is also a time dependent internal heat generation source term in each of the two equations representing heated sections.

There are also thermal energy equations for the two headers and the secondary side of the heat exchanger. Equation (a9) is the energy equation for the outlet header. The flows are assumed to be positive, as shown in Fig. A-3. If any of the leg flows are negative, the equation would have to be appropriately modified to use the upstream value of temperature. Equation (a10) is the expression for the updated outlet header temperature. The inlet header thermal energy equation is derived in a similar fashion.

$$mC_p \frac{T_{out}^n - T_{out}}{\Delta t} = \sum_{i=1,3} \dot{m}_i C_p \left[\alpha T_{i,5}^n + (1-\alpha)T_{i,5}\right] - \dot{m}_{Hx} C_p \left[\alpha T_{out}^n + (1-\alpha)T_{out}\right] \tag{a9}$$

$$T_{out}^n = \frac{\left[\frac{mC_p}{\Delta t} - \dot{m}_{Hx} C_p (1-\alpha)\right] T_{out} + \sum_{i=1,3} \dot{m}_i C_p \left[\alpha T_{i,5}^n + (1-\alpha)T_{i,5}\right]}{\frac{mC_p}{\Delta t} + \dot{m}_{Hx} C_p \alpha} \tag{a10}$$

Figure A-4 is a schematic of the heat transfer between the primary and secondary sides of the heat exchanger. Equation a11 is the thermal energy equation for the tube side of the heat exchanger, and Eq. a12 is the energy equation for the shell side. The shell side of the heat exchanger is assumed to exchange energy only with the tube side. The outer surface of the shell is assumed to be an adiabatic boundary. Equation (a13) is the expression for the heat transfer rate between the two sides of the heat exchanger. The heat transfer coefficient accounts for single-phase convective heat transfer on both sides of the heat exchanger

and conduction through the tube walls. The mass and specific heat for the secondary side of the heat exchanger are composites of both the metal and the liquid.

$$mC_p \frac{T_{Hx,2}^n - T_{Hx,2}}{\Delta t} = \dot{m}_{Hx} C_p \left[\alpha\left(T_{Hx,1}^n - T_{Hx,2}^n\right) + (1-\alpha)\left(T_{Hx,1} - T_{Hx,2}\right)\right] - \dot{Q}_{conv} \tag{a11}$$

$$\left(mC_p\right)_{sh} \frac{T_{sh}^n - T_{sh}}{\Delta t} = \dot{Q}_{conv} \tag{a12}$$

$$\dot{Q}_{conv} = h_{conv} A_{Hx} \left[\alpha T_{Hx,2}^n + (1-\alpha) T_{Hx,2} - \alpha T_{sh}^n - (1-\alpha) T_{sh}\right] \tag{a13}$$

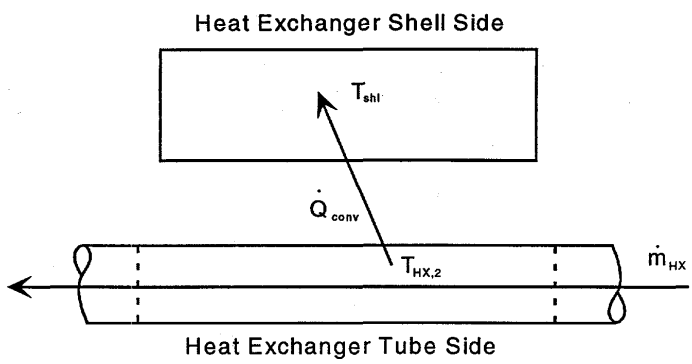

Figure A-4. Schematic of the heat exchanger showing the heat transfer to the secondary side.

APPENDIX B: BUOYANCY-ASSISTED AMD BUOYANCY-OPPOSED FRICTION FACTOR MULITPLIERS

To account for the influence of wall heating on the friction factors for flow through the vertical modules, results of an analytical study of fully developed laminar flow between vertical parallel plates were used (see Ref. [3]). A plot of the product of the friction factor and the Reynolds number versus the one-fourth power of a modified Rayleigh number was used to develop functional relations for mixed convection multipliers to friction factors. The modified Rayleigh number used is defined as

$$Ra = \frac{g\beta\left(\frac{dT_w}{dx}\right) D_H^4 \rho^2 \, Pr}{\mu^2} \tag{b1}$$

For fully developed flow with a constant wall heat flux, the wall and fluid axial temperature gradients are equal. The wall axial temperature gradient can, therefore, be expressed as a function of the wall power and the fluid mass flowrate (Eq. (b2)).

$$\frac{\Delta T}{L} = \frac{\dot{Q}_w}{L\dot{m}C_p} \tag{b2}$$

Substituting Eq. (b2) and the definition of the Prandtl number into the expression for the modified Rayleigh number results in Eq. (b3), the form of the modified Rayleigh number that is used in the NC model of the primary HR system. The Rayleigh number is directly

proportional to the deposited power in the fluid and inversely proportional to the mass flowrate. It expresses the relative importance of buoyancy in vertical mixed convection.

$$Ra = \frac{g\beta \dot{Q}_w D_H^4 \rho^2}{\dot{m}\mu L k} \qquad \text{(b3)}$$

Reference 3 presents results for the range of Rayleigh numbers to the one-fourth power from zero to twelve. Results are presented for both buoyancy-assisted and buoyancy- opposed flows. For buoyancy-opposed flow, results are presented for the Rayleigh number to the one-fourth-power range up to four. Beyond this point the buoyancy- opposed mixed convection friction behavior is not defined. From the results in Ref. [3], Darcy friction factor multiplier relations were developed. These relations are Eqs.(b4) through (b8), and they are shown graphically by the solid Jines in Fig. B-1. The curves are first-order continuous over the entire Rayleigh number to the one-fourth-power range shown. The curve for buoyancy-opposed flow at Rayleigh numbers to the one fourth power greater than four is simply conjecture, and it is included in the model to insure that a reasonable value of the friction factor multiplier is returned in all cases. Having first-order continuous constitutive relations in the model is desirable from a numerical perspective.

$$\phi \equiv \frac{f_{Mixed}}{f_{Laminar}} = 1.0 \quad \text{for} \quad Ra^{1/4} \le 1.5 \qquad \text{(b4)}$$

Buoyancy-Assisted Flow:

$$\phi = \begin{cases} e^{\left[C_1\left(Ra^{1/4}-1.5\right)^2 + C_2\left(Ra^{1/4}-1.5\right)^3\right]} & \text{for} \quad 1.5 < Ra^{1/4} \le 8.0 \\ e^{\left[C_3 + C_4\left(Ra^{1/4}-1.5\right)\right]} & \text{for} \quad Ra^{1/4} > 8.0 \end{cases} \qquad \text{(b5) and (b6)}$$

Buoyancy-Opposed Flow:

$$\phi = \begin{cases} e^{\left[C_5\left(Ra^{1/4}-1.5\right)^2 + C_6\left(Ra^{1/4}-1.5\right)^3 + C_7\left(Ra^{1/4}-1.5\right)^4\right]} & \text{for} \quad 1.5 < Ra^{1/4} \le 8.0 \\ 0.0416 & \text{for} \quad Ra^{1/4} \le 8.0 \end{cases} \qquad \text{(b7) and (b8)}$$

where:

$C_1 = 0.11815501$
$C_2 = -2.9378955 \times 10^{-3}$
$C_3 = -3.3784101$
$C_4 = 1.1636369$
$C_5 = -3.8259936 \times 10^{-1}$
$C_6 = 7.1433520 \times 10^{-2}$
$C_7 = -3.7145261 \times 10^{-3}$

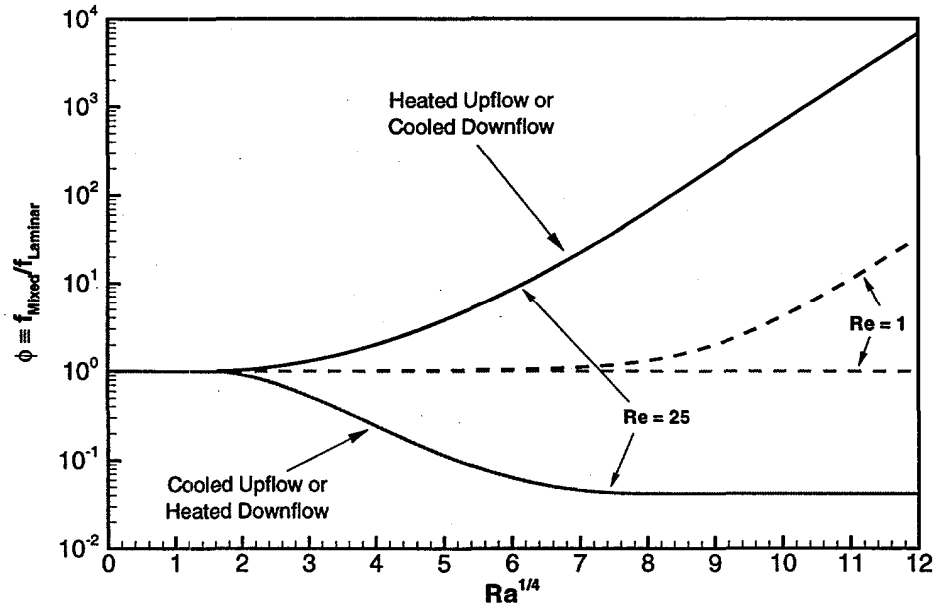

Figure B-1. Friction factor multipliers for buoyancy-assisted and buoyancy-opposed mixed convection in vertical channels.

The Rayleigh number is inversely proportional to the mass flowrate. If the Rayleigh number to the one-fourth power were not limited to a maximum value of twelve in the NC model, it could grow without bound during flow reversals. Even with this restriction on the value of the parameter, there will be a large discontinuity in the values of the friction factor multipliers as the flow direction reverses in a heated vertical passage. To prevent this discontinuity, Eq. (b9) modifies the friction factor multiplier when the Reynolds number is less than twenty-five. This equation interpolates non-linearly between the buoyancy-assisted and buoyancy-opposed values of the friction factor multiplier at a Reynolds number of twenty-five and a value of unity when the Reynolds number is zero. It can easily be seen that, with Eq. (b9), at a Reynolds number of twenty- five the friction factor multiplier is unaltered, and at zero the friction factor multiplier is unity. This equation insures that the friction factor and its first derivative are continuous as the flow reverses. The dotted lines in Fig. B-1 show the values of the friction factor multiplier at a Reynolds number of one.

$$\phi_{(Re\leq 25)} = 1 - \left[3 - 2\left(\frac{Re}{25}\right)\right]\left(\frac{Re}{25}\right)^2 + \left[3 - 2\left(\frac{Re}{25}\right)\right]\left(\frac{Re}{25}\right)^2 \phi \qquad \text{(b9)}$$